

RESEARCH ARTICLE

# Traditional Chinese Nootropic Medicine *Radix Polygalae* and Its Active Constituent Onjisaponin B Reduce $\beta$ -Amyloid Production and Improve Cognitive Impairments

Xiaohang Li<sup>1,2</sup>, Jin Cui<sup>1,2</sup>, Yang Yu<sup>3</sup>, Wei Li<sup>1,2</sup>, Yujun Hou<sup>1</sup>, Xin Wang<sup>1,2</sup>, Dapeng Qin<sup>3</sup>, Cun Zhao<sup>1,2</sup>, Xinsheng Yao<sup>3</sup>, Jian Zhao<sup>1,4\*</sup>, Gang Pei<sup>1,5\*</sup>

**1** State Key Laboratory of Cell Biology, Institute of Biochemistry and Cell Biology, Shanghai Institutes for Biological Sciences, Chinese Academy of Sciences, Shanghai, China, **2** Graduate School, University of Chinese Academy of Sciences, Chinese Academy of Sciences, Shanghai, China, **3** Institute of Traditional Chinese Medicine and Natural Products, College of Pharmacy, Jinan University, Guangzhou, China, **4** Translational Medical Center for Stem Cell Therapy, Shanghai East Hospital, School of Medicine, Tongji University, Shanghai, China, **5** School of Life Science and Technology, Collaborative Innovation Center for Brain Science, Tongji University, Shanghai, China

\* [gpei@sibs.ac.cn](mailto:gpei@sibs.ac.cn) (GP); [jzhao@sibs.ac.cn](mailto:jzhao@sibs.ac.cn) (JZ)



**OPEN ACCESS**

**Citation:** Li X, Cui J, Yu Y, Li W, Hou Y, Wang X, et al. (2016) Traditional Chinese Nootropic Medicine *Radix Polygalae* and Its Active Constituent Onjisaponin B Reduce  $\beta$ -Amyloid Production and Improve Cognitive Impairments. PLoS ONE 11(3): e0151147. doi:10.1371/journal.pone.0151147

**Editor:** Madepalli K. Lakshmana, Torrey Pines Institute for Molecular Studies, UNITED STATES

**Received:** October 5, 2015

**Accepted:** February 24, 2016

**Published:** March 8, 2016

**Copyright:** © 2016 Li et al. This is an open access article distributed under the terms of the [Creative Commons Attribution License](https://creativecommons.org/licenses/by/4.0/), which permits unrestricted use, distribution, and reproduction in any medium, provided the original author and source are credited.

**Data Availability Statement:** All relevant data are within the paper and its Supporting Information files.

**Funding:** This research was supported by the National Natural Science Foundation of China (31371419), Ministry of Health (2012BAI10B03) and Shanghai Municipal Commission for Science and Technology (13401900600, 14DZ1900402).

**Competing Interests:** The authors have declared that no competing interests exist.

## Abstract

Decline of cognitive function is the hallmark of Alzheimer's disease (AD), regardless of the pathological mechanism. Traditional Chinese medicine has been used to combat cognitive impairments and has been shown to improve learning and memory. *Radix Polygalae* (RAPO) is a typical and widely used herbal medicine. In this study, we aimed to follow the  $\beta$ -amyloid (A $\beta$ ) reduction activity to identify active constituent(s) of RAPO. We found that Onjisaponin B of RAPO functioned as RAPO to suppress A $\beta$  production without direct inhibition of  $\beta$ -site amyloid precursor protein cleaving enzyme 1 (BACE1) and  $\gamma$ -secretase activities. Our mechanistic study showed that Onjisaponin B promoted the degradation of amyloid precursor protein (APP). Further, oral administration of Onjisaponin B ameliorated A $\beta$  pathology and behavioral defects in APP/PS1 mice. Taken together, our results indicate that Onjisaponin B is effective against AD, providing a new therapeutic agent for further drug discovery.

## Introduction

Alzheimer's disease is a complex and currently incurable age-related neurodegenerative disease and is highly prevalent in aged cohorts worldwide [1]. It is the most common late-age mental failure in humans and currently exerts great economic and political pressure on modern society. A $\beta$  deposition, tau tangles and cognitive degeneration are the hallmarks of the disease [2], therefore reducing A $\beta$  production and improving cognitive function has been considered as an effective disease- and symptom-modifying therapeutic strategy.

The amyloid cascade hypothesis is supported by accumulating studies based on cell culture and animal experiments [3]. In amyloid hypothesis, the maturation, processing and degradation of APP and the consequential production and clearance of A $\beta$  initiate AD pathogenesis [4]. APP can be sequentially cleaved by BACE1 and  $\gamma$ -secretase [5, 6] and finally yield A $\beta$  species. This makes BACE1 and  $\gamma$ -secretase key-players in AD pathogenesis. In brains of Alzheimer's disease patients, large amounts of A $\beta$  are produced and aggregated, mainly in the hippocampus and prefrontal cortex, causing neuronal death and impairment of cognitive function [7, 8]. Thus, for the past two decades, to identify a solution for this devastating disease, researchers have focused on modulating BACE1 or  $\gamma$ -secretase activities. The cellular A $\beta$  level can be reduced, and cognitive function impairments have been shown to be ameliorated in transgenic AD model mice treated with secretase inhibitors or modulators [9]. However, treatments with these compounds have been discontinued because of severe adverse effects in recent clinical trials [10, 11]. Aside from functions in A $\beta$  generation, BACE1 and  $\gamma$ -secretase are also involved in multiple physiological processes including cell adhesion and Notch signaling. These accumulating evidences suggest that the strategy of directly inhibiting the enzymatic activity of BACE1 and  $\gamma$ -secretase may need to be optimized. APP and its proteolytic products undergo degradation via protein degradation pathways [12–14]. The proteasome is the major organelle for protein degradation in cells [15], and cleavage through this pathway reduces A $\beta$  production [16–18]. Furthermore, our previous work has shown that interfering with the interaction between BACE1 and  $\gamma$ -secretase, thereby blocking the sequential process and reducing A $\beta$  production, may have some advantages in modifying the disease [19].

Traditional Chinese medicine has long been used to treat dementia [20–23]. Among those historically used herbal drugs, *Radix Polygalae* (RAPO) has been demonstrated to exhibit nootropic activity [20, 24, 25]. Moreover, our previous data regarding the “Smart soup” containing *Rhizoma Acori Tatarinowii*, *Poria cum Radix Pini* and *Radix Polygalae* showed systematic beneficial effects against AD and RAPO function to decrease A $\beta$  production [24, 26]. Herein, we explored the major component(s) of RAPO and the related underlying mechanism.

## Materials and Methods

### Ethics Statement

All animal experiments were performed according to the National Institutes of Health Guide for the Care and Use of Laboratory Animals. The animal protocols were approved by the Biological Research Ethics Committee, Shanghai Institutes for Biological Sciences, Chinese Academy of Sciences. Effort was made to minimize animal pain and discomfort. The IACUC approved this research under the approval number SIBCB-NAF-14-002-S309-015.

### Animal

The APP<sup>swe</sup>/PS1 $\Delta$ E9 (APP/PS1) double-transgenic mice (JAX Stock No. 004462) brought from Jackson Laboratory express a chimeric mouse/human amyloid precursor protein (Mo/HuAPP695<sup>swe</sup>) and a mutant human Presenilin 1 (PS1 $\Delta$ E9). The mice were maintained and genotyped according to the Jackson Laboratory guidelines.

### Drug administration

The transgene-negative wild-type (WT) littermates were used as gender- and age-matched controls. RAPO-1-3 or Onjisaponin B was dissolved in vehicle (50% PEG400 in H<sub>2</sub>O). APP/PS1 and WT mice were chronically administered 200  $\mu$ l of Onjisaponin B (1 mg/ml), RAPO-1-

3 (15 mg/ml) or vehicle per 20 g body weight by oral gavage once per day from 4 to 7 months of age (n = 12 to 16 mice per group).

### Morris water maze

The Morris water maze analysis was performed as previously reported [27], and the animals were randomly numbered among genotypes and grouped for the test. The apparatus was a 120-cm-diameter circular pool filled with water containing small white plastic particles, with cues of four different shapes posted on four directions of the inner pool wall. The water temperature was maintained at  $23.0 \pm 0.5^\circ\text{C}$  and the room temperature at  $25.0 \pm 0.5^\circ\text{C}$  during the whole procedure. A transparent platform 11 cm in diameter was placed 1 cm below the water surface at a fixed position in the target quadrant. The training consisted of 4 trials per day for 7 consecutive days. On day 4, probe trials were conducted after the fourth training trial. On day 8, a single round of probe trial was performed. An automated tracking system (Ethovision XT software) was used to monitor the mouse swimming paths and other parameters.

### Immunohistochemistry and image analysis

The mice were anesthetized and transcardially perfused with phosphate-buffered saline (PBS) buffer and then with 4% paraformaldehyde (PFA). Brain cryo-sections (30  $\mu\text{m}$  thick) were prepared and immunostained using 6E10 for amyloid plaques and GFAP for astrocytes. Images were captured using a Carl Zeiss Z1 microscope (Zeiss). Quantification was performed using Image-Pro Plus 5.1 software (Media Cybernetics). Ten to fifteen coronal sections were analyzed per mouse.

### Compounds, reagents and antibodies

Onjisaponin B (purity > 98%) was purchased from Biopurity, and RP granules were purchased from Jiangyin Tianjiang Pharmaceutical Co., Ltd. L-685,458 (purity > 96%) and (S)-(+)-ibuprofen (purity > 99%) were purchased from Sigma, DAPT (purity > 99%) was purchased from Selleck and BACE1 inhibitor IV (purity > 98%) was purchased from Calbiochem. E2012 was synthesized by Ginkgo Pharma. MG132 (purity > 97%) was purchased from Selleck and lactacystin (purity > 98%) from Santa Cruz. CellTiter-Glo was purchased from Promega. Fugene HD and Effectene Transfection Reagent were purchased from Roche and QIAGEN, respectively. Immunoblotting was performed with the following antibodies: anti-ADAM10 (a Disintegrin and metalloproteinase domain-containing protein 10) C-term (Sigma); anti-PS1 (1–65) (EMD); anti-BACE1 N-term (Abgent); anti-APP-CTF (Sigma); anti-Flag (Sigma); anti-sAPP $\alpha$  (secreted Amyloid Precursor Protein- $\alpha$ ) (IBL); anti-sAPP $\beta$  (secreted Amyloid Precursor Protein- $\beta$ ) (IBL); anti-HA (Sigma); anti-c-Myc (Santa Cruz); anti-NICD (Notch intracellular domain) (Cell Signaling); anti-E-Cadherin-CTF (BD Transduction Laboratories); anti-APLP1 (APP-like protein 1) C-Terminal (643–653) (Calbiochem). Secretase activity assays were performed with anti-A $\beta$ 40 (EMD Millipore) and anti-A $\beta$  (82E1, IBL). Immunohistochemistry was performed with anti-A $\beta$ , 1–16, 6E10 (Covance) and anti-GFAP (Glial fibrillary acidic protein) (Dako).

### Cell culture and plasmids

HEK293T, HEK293 and A431 cells were previously purchased from ATCC, and HEK293MSR cells were a kind gift from Sanofi-Aventis Research and Development. All cell lines were maintained under the same condition as described previously [19]. In detail, HEK293T, HEK293MSR, HEK293/APP<sup>swe</sup> and A431 were cultured in Dulbecco's modified Eagle's

medium (DMEM) with 10% (w/v) heat-inactivated fetal bovine serum in a humidified incubator with 5% CO<sub>2</sub>/95% air (v/v) at 37°C. HEK293 cells were cultured in MEM under the same condition. The Swedish mutant form of APP was transfected into HEK293 using Fugene HD (Roche) following the manufacturer's instructions. A cell line stably expressing Swedish mutant APP was established in the presence of 1 mg/ml G418. Penicillin-Streptomycin solution (Life Technologies) was added according to the manual. All constructs were the same as reported previously and were verified by sequencing [19, 28].

## ELISA for A $\beta$

HEK293/APP<sub>swe</sub> cells were treated with chemicals at the indicated concentrations and durations. The conditioned medium was then collected and subjected to a sandwich ELISA for the total A $\beta$  level. Human A $\beta$ 40 and A $\beta$ 42 in APP/PS1 mouse brains were extracted as previously reported [29] and measured with human A $\beta$  ELISA kits according to the manufacturer's guidelines. ELISA kits for total human A $\beta$ , human A $\beta$ 40 and human A $\beta$ 42 were obtained from ExCell Bio.

## *In vitro* BACE1 and $\gamma$ -secretase assays

Total membrane fractions were extracted from 293T cells or APP/PS1 mouse brain and used in ELISA-based secretase assays or fluorogenic substrate assays to measure BACE1 or  $\gamma$ -secretase activity. Fluorogenic substrate assays and the ELISA-based  $\gamma$ -secretase assay were carried out as previously reported [30, 31]. For the ELISA-based BACE1 assay, membrane fractions of HEK293T cells were collected after lysis in buffer A. Supernatants containing 20 mg protein were centrifuged at 25000 g for 1 hour. The resulting membrane pellets were then resuspended in BACE1-assay buffer (50 mM sodium acetate, pH 4.5 and 0.5 mM biotinylated APP-TM peptide). After being incubated at 37°C for 30 minutes, the reaction mixtures or biotinylated standard peptides DK-16 were neutralized by Tris-Na<sub>2</sub>HPO<sub>4</sub> buffer and added into streptavidin-coated 96-well plates (Pierce) and incubated at room temperature for one hour. Anti-A $\beta$  82E1 antibodies (IBL) were added to the plate and then incubated for another hour. After three washes, horseradish peroxidase-labeled anti-mouse antibodies were added, and the plates were incubated for one hour. Ultra-TMB (Pierce) was used as the substrate for horseradish peroxidase and the absorbance at 450 nm was recorded. Concentrations of samples were calculated according to standard curves. APP-TM peptide (amino acid sequence: SGLTNIKTEEISEVNL DAEFRHDSGYEVHHQK-biotin) and DK-16 (amino acid sequence: DAEFRHDSGYEVHHQK-biotin) were synthesized by GL Biochem.

## Secretase substrate processing assays

HEK293/APP<sub>swe</sub> cells or HEK293T cells transiently transfected with myc-Notch $\Delta$ E or PSGL1-HA were treated with chemicals for 4 hours, and membrane fractions or total lysates were analyzed for APP-CTF, NICD and PSGL1-CTF levels. Culture medium from HEK293/APP<sub>swe</sub> cells was subjected to Western blotting analysis for sAPP $\alpha$  and sAPP $\beta$  and to ELISA analysis for total A $\beta$ . The *in vitro* C99 assay was carried out as described previously [32]. The *in vitro* APP processing assay was performed using the membrane fraction of HEK293/APP<sub>swe</sub> cells incubated with the indicated chemicals *in vitro* at 37°C for 2 hours and then subjected to Western blot for APP-CTF analysis. Membrane fractions or total lysates of mouse brain were extracted and subjected to Western blotting analysis for ADAM10, BACE1, PS1, APLP1 and its CTF, and E-Cadherin CTFs. Flotillin or Actin was blotted as a loading control.

## Statistical analysis

All experiments were repeated at least three times. All data are presented as the mean  $\pm$  s.e.m. and analyzed using GraphPad Prism 6.01 (San Diego, CA, USA). The unpaired Student's *t*-test was used for comparisons of two groups. Group differences were analyzed with one-way analysis of variance (ANOVA). The results of Morris water maze hidden platform training were analyzed using two-way ANOVA. Differences were considered significant when  $p < 0.05$ .

## Results

### Systematic fractionation identifies RAPO-1-3 as the active fraction of RAPO that reduces A $\beta$ production

In our previous study, we showed that *Radix Polygalae* reduced A $\beta$  generation *in vivo* and *in vitro* [26]. To identify the active components, we first separated RAPO into 3 fractions using an ethanol-water gradient (Fig 1A). The concentrations of the fractions were calculated according to the yield and are presented as weight/volume (w/v) of original raw material. The concentrations of the different RAPO fractions applied to HEK293/APPswe cells are 0.1, 0.3 and 1 mg/ml (relative RAPO concentration). This relative concentration is converted based on the yield of each fractionation step. For example, according to the fractionation scheme, RAPO-1 is composed of 10.1588% dry weight of RAPO ( $43.6\% \times 23.3\% = 10.1588\%$ ), and 1 mg/ml (relative to RAPO) of RAPO-1 is equivalent to 0.1 mg/ml (actual concentration). We then treated HEK293/APPswe cells with various concentrations of each fraction. HEK293/APPswe cells stably overexpress human APP protein carrying a Swedish mutant (K595N/M596L) and show elevated A $\beta$  secretion [33]. Medium from HEK293/APPswe cells treated with RAPO fractions was collected to detect the total A $\beta$  level using a sandwich ELISA. Meanwhile, cells were lysed and subjected to the CellTiter-Glo assay to evaluate cell viability. The 8-hour treatment with RAPO-1 or RAPO-2 did not affect cell viability, whereas RAPO-3 reduced cell viability to 48% (S1A Fig). Compared to vehicle treatment, treatment with either RAPO-1 or RAPO-3 markedly reduced the A $\beta$  level in the conditioned medium, by 48% and 90%, respectively (S1A Fig). To test whether the A $\beta$ -reducing activity and cytotoxicity might be separated, we further fractionated RAPO-1 and RAPO-3 into three sub-fractions (Fig 1A). The cell viability was severely compromised upon RAPO-3-2 treatment, decreasing by 68% (S1B Fig), whereas the fraction RAPO-1-3 reduced A $\beta$  generation without obvious cytotoxicity (S1B Fig). These results indicate that RAPO-1-3 is the representative fraction of RAPO that reduces A $\beta$  production without affecting cell viability. Therefore, we focused on RAPO-1-3 in our further studies.

We then tested the *in vivo* efficacy of RAPO-1-3. It has been reported that APP/PS1 double transgenic mice begin to display accumulated A $\beta$  plaque deposition in the hippocampus and cortex, as well as age-dependent deficits in cognitive function at 6 months of age [34–36]. We chronically administered RAPO-1-3 to APP/PS1 mice. Gender- and age-matched APP/PS1 transgenic mice and their transgene-negative littermates were grouped and treated with RAPO-1-3 (0.15 g/kg/day) or Vehicle (50% PEG400 in distilled water) by oral gavage. During the drug administration, animals' body weights were recorded. The body weights in the RAPO-1-3 group showed no significant change compared to that of the vehicle group (data not shown), suggesting that there was no obvious toxic effect of the treatment. Three months later, the Morris Water Maze analysis was performed to evaluate the spatial learning and reference memory of the animals [27, 37, 38]. There was no obvious difference among animals in swimming distance or velocity (Fig 1E), implying that RAPO-1-3 treatment did not change mouse locomotor activity. As shown in Fig 1B, consistent with previous reports, APP/PS1 mice exhibited significantly impaired learning and memory ability compared to their wild-type

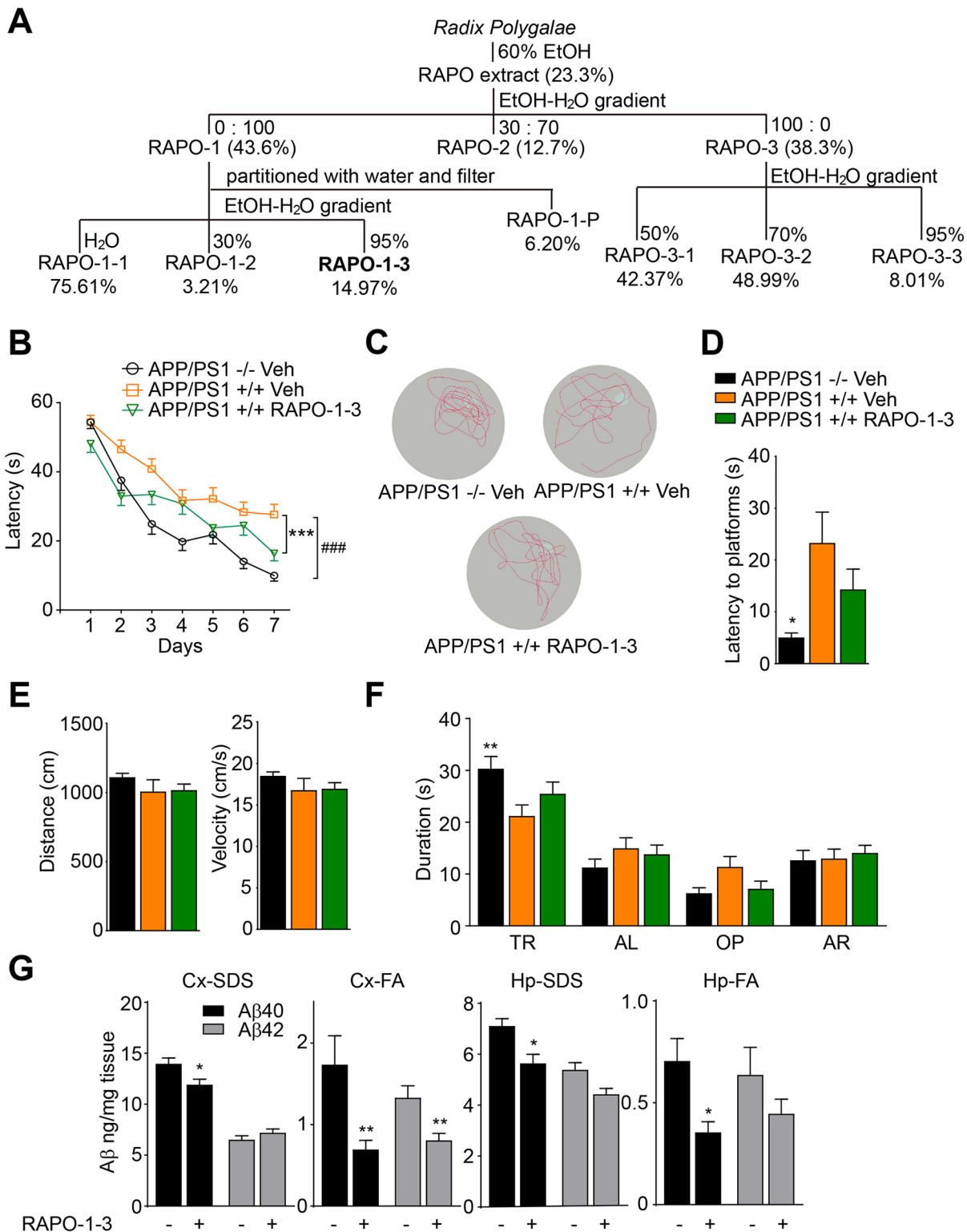


**Fig 1. Systemic fractionation identifies RAPO-1-3 as the active fraction of RAPO that reduces A $\beta$  production.** (A) The extraction and fractionation scheme of RAPO. (B) RAPO-1-3 significantly reverses the spatial memory deficit of AD mice. (C) Representative tracks of each group of mice in probe trial test at day 8. (D) The latency to platform in probe trial for each group of mice at day 8. (E) No differences in the swimming distance and velocity among the groups. (F) The time spent by mice in the target quadrant. (G) SDS-soluble and FA-soluble A $\beta$ 40 and A $\beta$ 42 levels in the mouse hippocampi and cortices were measured by sandwich ELISA and normalized to control. Data are presented as the mean  $\pm$  s.e.m. \*  $p < 0.05$ , \*\*  $p < 0.01$  and \*\*\*  $p < 0.001$ . Two-way ANOVA with Bonferroni's multiple comparison test (B, F), one-way ANOVA with Bonferroni's multiple comparison test (D, E) and two-tailed  $t$ -test (G).

doi:10.1371/journal.pone.0151147.g001

littermates in the hidden platform phase (Veh APP/PS1 -/- vs. Veh APP/PS1 +/+,  $p < 0.0001$ ) [36]. Interestingly, these spatial learning and memory deficits of APP/PS1 mice were ameliorated by chronic administration of RAPO-1-3 (RAPO-1-3 APP/PS1 +/+ vs. Veh APP/PS1 +/+,  $p < 0.0001$ ). During the probe trial at day 8, the mice treated with RAPO-1-3 took less time to reach the position of the platform (RAPO-1-3 APP/PS1 +/+ vs. Veh APP/PS1 +/+,  $p = 0.2479$ ) (Fig 1D), spent more time in the target quadrant (RAPO-1-3 APP/PS1 +/+ vs. Veh APP/PS1 +/+,  $p = 0.2116$ ) (Fig 1F), and crossed more frequently within the platform area (Fig 1C). These data indicate that RAPO-1-3 effectively ameliorates the spatial learning and reference memory deficiency of APP/PS1 transgenic mice. Soluble A $\beta$  oligomers are deleterious and correlate to cognitive deficits in Alzheimer's disease [39, 40]. Hence, SDS-soluble and FA-soluble A $\beta$ 40 and A $\beta$ 42 in mouse cortices and hippocampi were quantified by sandwich ELISA. SDS-soluble A $\beta$ 40 and A $\beta$ 42 were moderately reduced in the cortex and hippocampus, while FA-soluble A $\beta$ 40 and A $\beta$ 42 were significantly reduced (Fig 1G). These data indicate that RAPO-1-3 functions as the active fraction of RAPO that reduces A $\beta$  production *in vivo* and *in vitro*, as well as attenuating the learning and memory deficits in APP/PS1 mice.

### RAPO-1-3 and Onjisaponin B reduce A $\beta$ production without affecting BACE1 or $\gamma$ -secretase activity

A $\beta$  is produced by sequential processing of APP by BACE1 and  $\gamma$ -secretase [5, 41–44]. We next explored the activity of these two secretases. Using an ELISA-based secretase activity assay [45], we tested whether these active fractions directly inhibited secretase activity. As shown in Fig 2A, while BACE1 inhibitor IV (BSI IV) significantly inhibited BACE1 activity, and  $\gamma$ -secretase inhibitor (GSI) L685458 inhibited  $\gamma$ -secretase activity, RAPO fractions showed no significant effect on either secretase (Fig 2A). We further monitored the processing of other BACE1 and  $\gamma$ -secretase substrates in the presence of RAPO-1-3. P-selectin glycoprotein ligand-1 (PSGL1), a high-affinity counter-receptor for P-selectin that is responsible for tethering myeloid cells and stimulating T lymphocytes to activate platelets or endothelia, is another substrate of BACE1 [46, 47]. We investigated whether PSGL1 cleavage is affected by RAPO-1-3 using western blotting. The abundance of the C-terminal fragment of PSGL1 was significantly decreased in the presence of BSI IV and increased with transient overexpression of BACE1 as reported previously [47]. However, neither RAPO-1-3 nor RAPO-3-2 treatment altered the PSGL1 processing pattern (Fig 2B). Moreover, NICD level was markedly reduced by L685458, while the treatment with BSI IV or RAPO fractions did not interfere with the Notch $\Delta E$  cleavage pattern (Fig 2C). These data suggest that RAPO-1-3 harbors A $\beta$ -reducing activity and shows no direct inhibitory effects on the activities of BACE1 or  $\gamma$ -secretase.

To further identify the active constituents in RAPO-1-3, HPLC analysis was performed (data not shown). Several major chemical constituents were enriched in the RAPO-1-3 fraction. For detailed inspection, we performed UPLC-ESI-MS. Acyl saponins that possess the same saponin aglycone, similar glycosyl, and substituted groups account for approximately 12.8% of RAPO-1-3 (S2A–S2C Fig). Among them, Onjisaponin B was the relative abundant and characteristic one. The crude RAPO-1-3 extracts contained ~2.4% (w/w) Onjisaponin B according to the chromatogram of RAPO-1-3 and UPLC-Q/TOF-MS chromatogram of the pure standard compound (S2D–S2F Fig and S2 Table). In fractions adjacent to RAPO-1-3, only a trace amount of Onjisaponin B was detected. To determine whether Onjisaponin B functioned as RAPO-1-3, we assessed Onjisaponin B for its A $\beta$  reducing activity using the HEK293/APP<sub>swe</sub> cell line. Tenuifolin was compared in parallel as a core structure control. Indeed, Onjisaponin B exhibited comparable A $\beta$  reducing activity with RAPO-1-3 with an IC<sub>50</sub> of 10  $\mu$ M, while Tenuifolin showed no effect (Fig 2D and 2E). Neither Onjisaponin B nor

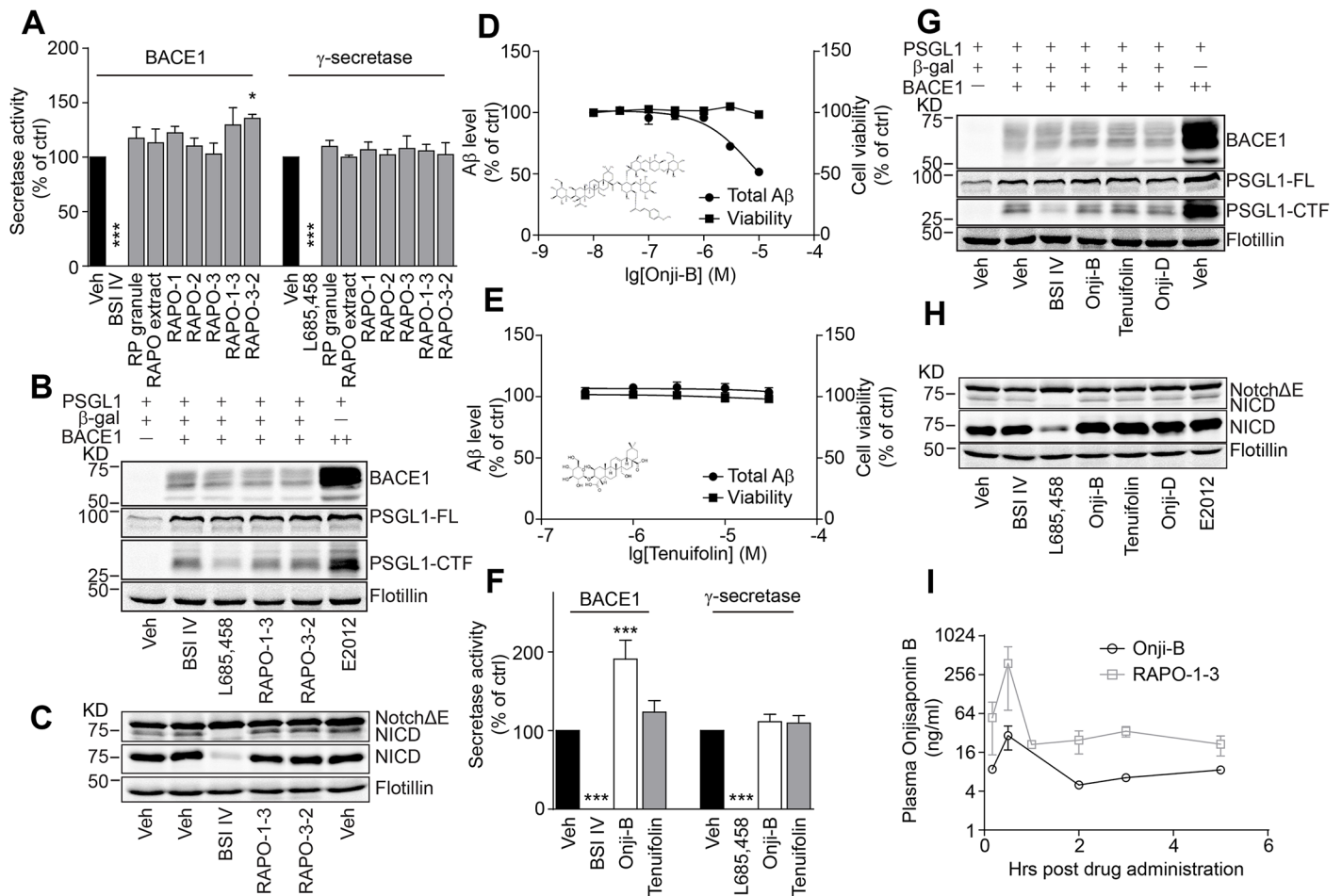


**Fig 2. RAPO-1-3 and Onjisaponin B reduce A $\beta$  generation without affecting the enzymatic activity of BACE1 or  $\gamma$ -secretase.** (A) RAPO fractions (1 mg/ml) do not alter the activity of BACE1 or  $\gamma$ -secretase. (B-C) Neither RAPO-1-3 nor RAPO-3-2 (1 mg/ml) changes the processing of PSGL1 by BACE1 (B) or of Notch by  $\gamma$ -secretase (C). Onjisaponin B (D) but not Tenuifolin (E) reduces A $\beta$  production without inhibiting BACE1 or  $\gamma$ -secretase (F) activity. (G-H) Neither Onjisaponin B nor Tenuifolin (10  $\mu$ M) alters the processing of PSGL1 by BACE1 (G) or of Notch by  $\gamma$ -secretase (H). (I) Onjisaponin B concentration within mouse plasma after the acute administration of RAPO-1-3 or Onjisaponin B. In the figures, Onji-B stands for Onjisaponin B. Data are presented as the mean  $\pm$  s.e.m. \*  $p < 0.05$ , \*\*  $p < 0.01$  and \*\*\*  $p < 0.001$ . One-way ANOVA with Bonferroni's multiple comparison test (A, F).

doi:10.1371/journal.pone.0151147.g002

Tenuifolin showed obvious cytotoxicity during the treatment as revealed by the CellTiter-Glo test (Fig 2D and 2E). Then, we examined whether Onjisaponin B affected BACE1 and  $\gamma$ -secretase activities. Surprisingly, Onjisaponin B enhanced BACE1 activity in the ELISA-based BACE1 activity assay (Fig 2F). However, the western blots for the processing patterns of the physiological BACE1 substrates APP and PSGL1 were not altered upon Onjisaponin B treatment (Figs 2G and 3B). Meanwhile,  $\gamma$ -secretase activity was not changed upon Onjisaponin B treatment (Fig 2F). Furthermore, we examined the effects of these compounds on Notch $\Delta$ E processing. We did not observe effects of Onjisaponin B on the processing of the  $\gamma$ -secretase substrate Notch $\Delta$ E (Fig 2H). Thus, the function of Onjisaponin B resembles that of RAPO-1-3, reducing A $\beta$  production without directly interfering with BACE1 or  $\gamma$ -secretase enzymatic activity. Moreover, unlike the  $\gamma$ -secretase modulator (GSM) ibuprofen or the GSI Compound E, Onjisaponin B did not affect the efficiency of PS1 internal FRET [28] (S4C Fig), suggesting that Onjisaponin B is neither a GSM nor a GSI. Next, we acutely administered RAPO-1-3 (0.15 g/kg/day) or Onjisaponin B (10 mg/kg/day) to C57BL/6 mice. Plasma was collected after 10



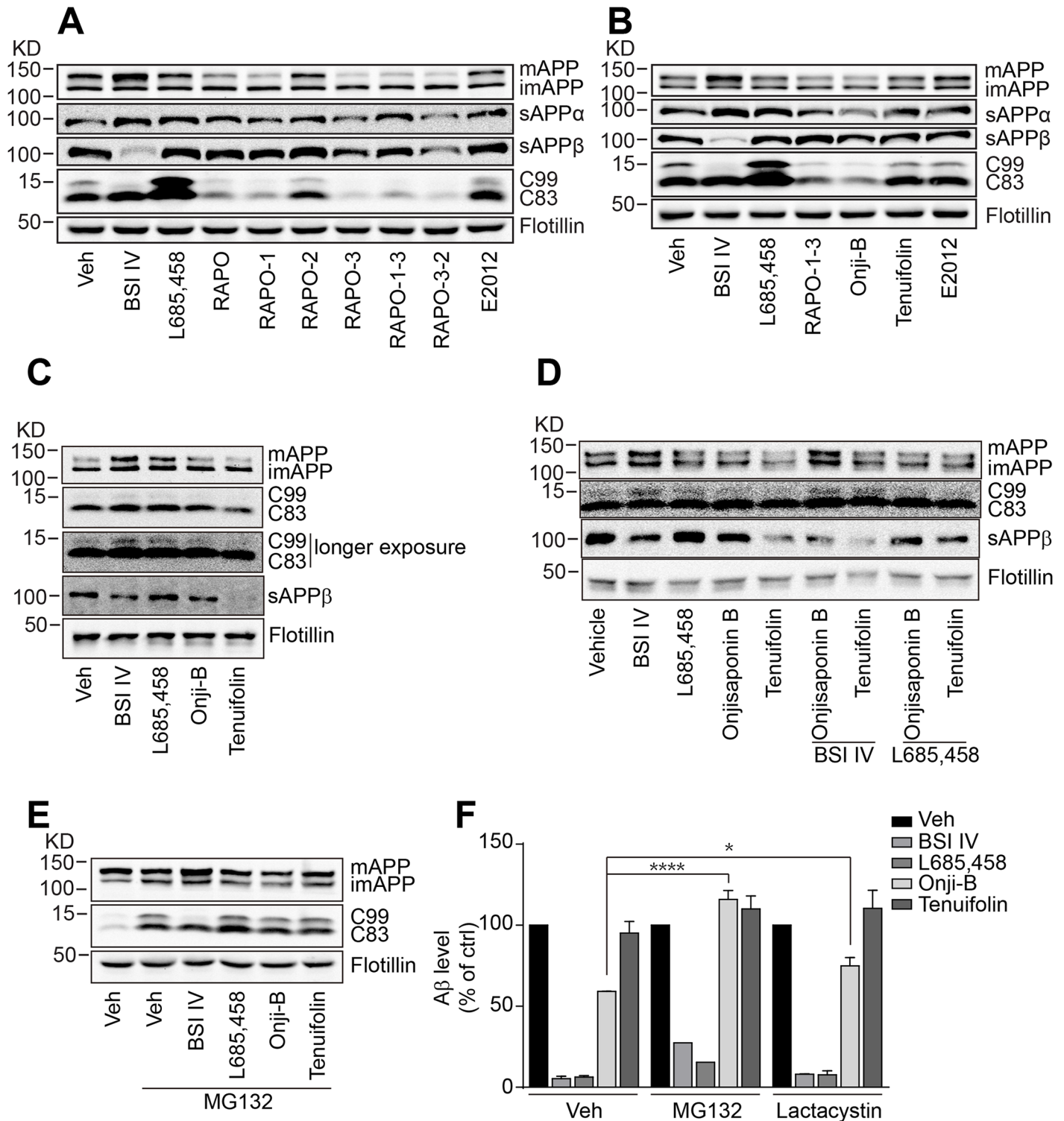


**Fig 3. Onjisaponin B promotes APP degradation.** (A-B) RAPO, RAPO fractions (1 mg/ml) (A) and Onjisaponin B (10  $\mu$ M) (B) reduce mature APP levels in HEK293-APPsw cells. (C) Generation of sAPP $\beta$  in the presence of 10  $\mu$ M Onjisaponin B or Tenuifolin in BACE1-assay buffer. (D) Mature APP was accumulated in detergent-soluble membrane fractions treated with 10  $\mu$ M BSI IV together with Onjisaponin B. (E-F) The proteasome inhibitor MG132 (10  $\mu$ M) prevents the reduction of mature APP (E) and A $\beta$  generation (F) by Onjisaponin B. (F) The proteasome inhibitor lactacystin (20  $\mu$ M) partially blocks the A $\beta$  reduction by Onjisaponin B. Data are presented as the mean  $\pm$  s.e.m. \*  $p < 0.05$ , \*\*  $p < 0.01$  and \*\*\*  $p < 0.001$ . Two-way ANOVA with Bonferroni's multiple comparison test (F).

doi:10.1371/journal.pone.0151147.g003

minutes, 30 minutes, 1 hour, 2 hours, 3 hours, 5 hours and 24 hours, and the concentration of Onjisaponin B in the plasma was detected. Plasma from the vehicle-treated mice were also collected and measured as background signal. Onjisaponin B was detectable with either RAPO-1-3 or Onjisaponin B treatment. The level of Onjisaponin B was approximately 4 times higher in the plasma of RAPO-1-3-treated mice than in that of the Onjisaponin B-treated group (Fig 2I).

## RAPO-1-3 and Onjisaponin B promote APP degradation

Studies show that interference with APP metabolism alters A $\beta$  production [16, 18, 48–51]. Thus, we monitored the APP cleavage pattern on western blots. Treatment with BSI IV completely abolished the production of sAPP $\beta$  and C99 and led to the accumulation of mature APP and C83. GSI L685,458 treatment caused the accumulation of C99 and C83, while the GSM E2012 exerted little effect on any of the APP metabolic products (Fig 3A). Conversely, treatment with RAPO, RAPO-1 or RAPO-1-3 led to a reduction in the level of full-length mature APP, and accordingly the protein levels of the cleavage products (including sAPP $\alpha$ , C83, sAPP $\beta$  and C99), while the immature APP level remained unchanged (Fig 3A). Onjisaponin B treatment resulted in a similar APP processing pattern (Fig 3B) as that of RAPO-1-3. Nevertheless, neither BACE1 expression nor its maturation changed significantly upon Onjisaponin B treatment (S3A Fig). These data suggest that Onjisaponin B may not reduce the cellular A $\beta$  level by blocking APP maturation. To test whether Onjisaponin B inhibited APP or secretase expression, we performed quantitative RT-PCR analysis. As shown in S3C Fig, we found no obvious differences among the mRNA levels of those proteins. Then, we tested whether it was the alteration of APP protein levels that led to the reduction of A $\beta$  production. The *in vitro* APP processing in the presence of active BACE1 was monitored. HEK293/APPSwe cell membrane fractions were extracted and incubated with the indicated compounds for 2 hours in BACE1-assay buffer. Treatment with BSI IV completely blocked sAPP $\beta$  generation and caused the accumulation of full-length mature APP and C99, while GSI L685,458 did not change the sAPP $\beta$  level but caused minor accumulation of APP and C99 (Fig 3C). However, both treatment with either Onjisaponin B or Tenuifolin reduced the level of sAPP $\beta$  while leaving the level of full-length APP unchanged (Fig 3C). Further, in the presence of Onjisaponin B together with BSI IV, the full-length mature APP accumulated to a level comparable to BSI IV alone, whereas the level of sAPP $\beta$  was decreased (Fig 3D). Co-treatment with L685,458 and Onjisaponin B showed no synergetic effect compared to L685,458 treatment alone (Fig 3D). Moreover, an *in vitro*  $\gamma$ -secretase activity analysis showed that the AICD production was not affected by Onjisaponin B treatment (S3B Fig). These data suggest that Onjisaponin B reduced A $\beta$  production neither by the direct inhibition of secretase activities nor by modulating protein expression. The proteasome proteolytic pathway has also been shown to be involved in the degradation of full-length APP [13, 52, 53]. Thus, we treated HEK293/APPSwe cells with BSI IV or L685,458 in the presence of the proteasome inhibitor MG132 and monitored the APP processing pattern. Consistent with previous reports [54], MG132 showed no obvious effect on the APP processing pattern in the presence of BACE1 or  $\gamma$ -secretase inhibitors (Fig 3E). Interestingly, the decreases in full-length mature APP and subsequently in C99 and C83 by Onjisaponin B were partially rescued in the presence of MG132 (Fig 3E). The A $\beta$  levels of the cells treated with MG132 and Onjisaponin B were comparable to those of the cells treated with MG132 alone (Fig 3F). To rule out the possibility that the rescue by MG132 was due to its GSI-like activity, we tested another, more specific proteasome inhibitor, lactacystin, which has been reported to show no GSI-like activity even at 100  $\mu$ M [55]. As shown in Fig 3F, the A $\beta$  levels of the cells treated with Onjisaponin B in the presence of lactacystin were significantly higher than those of the cells treated with Onjisaponin B alone. Together, these data indicate that

Onjisaponin B and the active fractions of RAPO reduce A $\beta$  production by promoting APP degradation through the proteasome pathway.

Additionally, as we recently reported that blocking the PS1/BACE1 interaction could also contribute to reduced production of A $\beta$  [19], we tested whether Onjisaponin B possessed a similar inhibitory activity. Co-immunoprecipitation analysis of PS1 and BACE1 was performed. As shown in [S4A Fig](#), Onjisaponin B interfered with the interaction between PS1 and BACE1. Further, FRET [19] ([S4B Fig](#)) and Split-TEV assay [19, 56] ([S4D Fig](#)) also showed that Onjisaponin B reduced the interaction between PS1 and BACE1. These data indicate that Onjisaponin B may possess multiple functions to reduce A $\beta$  production.

## Onjisaponin B ameliorates cognitive impairments in APP/PS1 mice

Because Onjisaponin B demonstrated the functions of RAPO-1-3 and reduced A $\beta$  production at the cellular level, we further tested whether Onjisaponin B was effective *in vivo*. We chronically administered Onjisaponin B to APP/PS1 mice. The drug administration began prophylactically at 4 months of age. Gender- and age-matched APP/PS1 transgenic mice and their WT littermates were grouped and treated with Onjisaponin B (10 mg/kg/day) or Vehicle (50% PEG400 in distilled water) by oral gavage. During Onjisaponin B administration, animals' body weights were recorded and no significant differences were observed among the groups ([S5A Fig](#)), showing that there were no obvious toxic effects in mice. After three months of drug administration, the mice were subjected to the Morris Water Maze analysis to evaluate their spatial learning and reference memory ability. The swimming distance and velocity remained at comparable levels among different groups of mice ([Fig 4C](#)), implying that treatment with Onjisaponin B does not alter mouse locomotor activity. As shown in [Fig 4A](#), consistent with previous results, APP/PS1 mice exhibited significantly impaired learning and memory ability in the hidden platform phase (Veh APP/PS1  $-/-$  vs. Veh APP/PS1  $+/+$ ,  $p < 0.0001$ ). This spatial learning and memory deficit in APP/PS1 mice was ameliorated by chronic administration of Onjisaponin B (Onji-B APP/PS1  $+/+$  vs. Veh APP/PS1  $+/+$ ,  $p = 0.0002$ ). During the probe trial on day 8, the mice treated with Onjisaponin B were faster in reaching the position of the platform ([S5B Fig](#)), spent more time in the target quadrant ([S5C Fig](#)), and crossed slightly more frequently within the platform area ([Fig 4B](#)) than the vehicle-treated APP/PS1  $+/+$  ones. These data indicate that Onjisaponin B effectively ameliorates the spatial learning and reference memory deficiency of APP/PS1 transgenic mice.

Along with the AD-like symptoms, APP/PS1 mice develop cerebral amyloidosis [57, 58]. Hence, a histological analysis was performed to assess their AD-like pathology. Brains of mice treated with Onjisaponin B exhibited significantly lower numbers of 6E10-positive A $\beta$  plaque and reduced plaque area compared to those of the vehicle-treated ones ([Fig 4D](#) and [S5D Fig](#)). SDS-soluble and FA-soluble A $\beta$ 40 and A $\beta$ 42 in mouse cortex and hippocampus were also monitored by ELISA. As shown in [Fig 4E](#), SDS-soluble A $\beta$ 40 and A $\beta$ 42 levels were moderately reduced in cortical and hippocampal extracts of the Onjisaponin B-treated group, while the levels of FA-soluble A $\beta$ 40 and A $\beta$ 42 were significantly reduced. Further assays of secretase activity revealed that none of the activities ([Fig 4F](#)) or the expression levels ([Fig 4G](#)) of BACE1 or  $\gamma$ -secretase in the brain extracts of the Onjisaponin B-treated mice altered. Moreover, the processing of other secretase substrates, i.e., APLP1 and E-cadherin, were also similar in mouse brain samples ([Fig 4H](#)). These data indicate that Onjisaponin B possesses *Radix Polygalae* activity and may ameliorate A $\beta$  pathology *in vivo*.

## Discussion

Drugs designed for Alzheimer's disease currently mostly focus on reducing A $\beta$  levels, which appears to be very challenging [59]. Direct inhibitors of secretases effectively inhibited A $\beta$

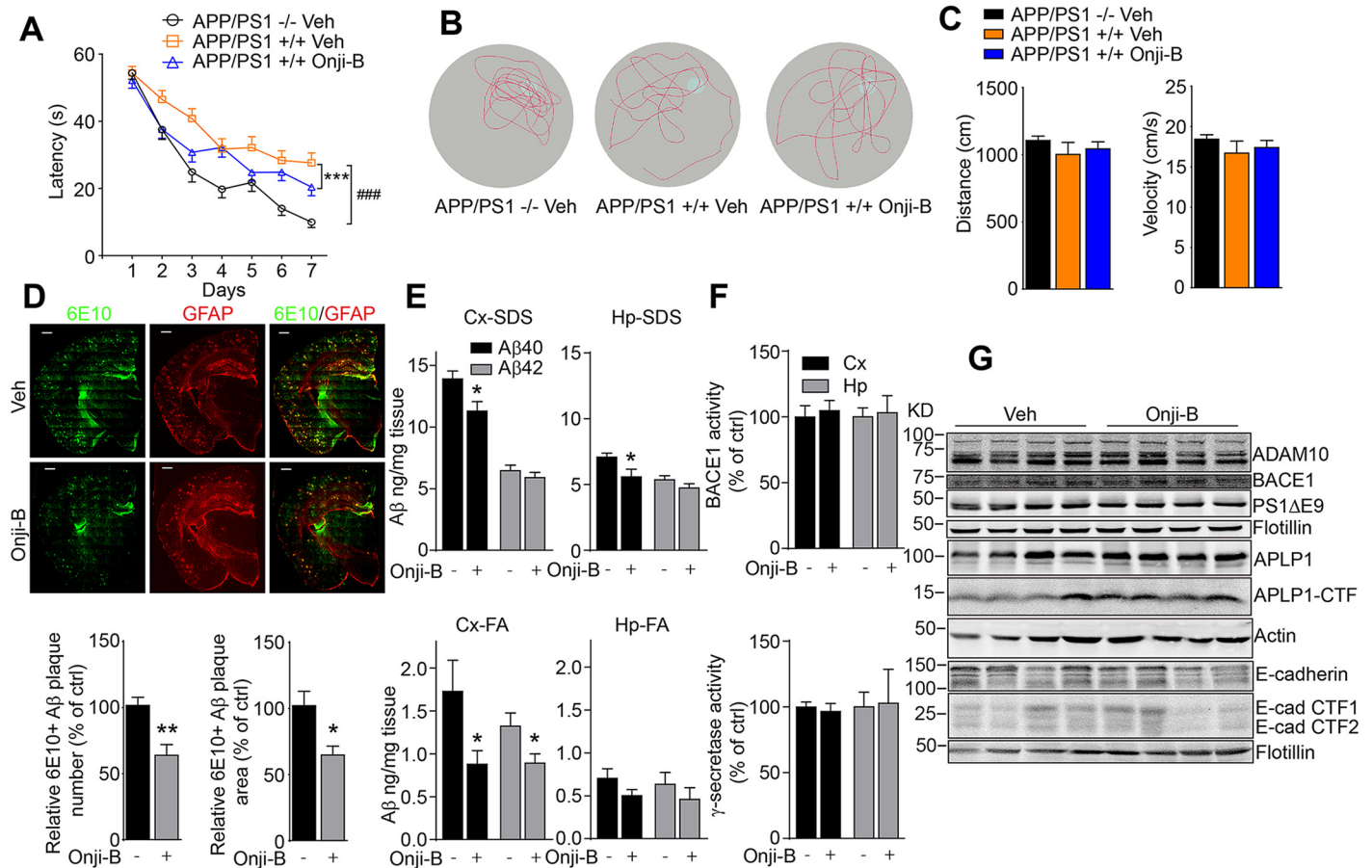


**Fig 4. Onjisaponin B ameliorates cognitive impairments in APP/PS1 mice.** (A) Onjisaponin B significantly attenuates spatial memory deficits of AD mice in the Morris Water Maze test. (B) Representative tracks of each group of mice in the probe trial test at day 8. (C) The swimming distance and velocity of mice. (D) Representative images of Aβ plaques in APP/PS1 mice immunostained with the Aβ antibody 6E10 in coronal mouse brain cryo-sections (n = 6 per group). The number and area of Aβ plaques, which are immunoreactive to 6E10, were quantified from entire brain sections using Image-Pro Plus 5.1 software (Media Cybernetics). Ten to fifteen coronal sections per mouse were analyzed. (E) SDS-soluble and FA-soluble Aβ40 and Aβ42 levels in mouse hippocampus and cortex measured by ELISA. (F) Mouse hippocampal and cortical BACE1 and γ-secretase activities and (G) Western blot analysis of cortical protein extracts with indicated antibodies. Data are presented as the mean ± s.e.m. \* p < 0.05, \*\* p < 0.01 and \*\*\* p < 0.001. Two-way ANOVA with Bonferroni's multiple comparison test (A), one-way ANOVA with Bonferroni's multiple comparison test (C) and two-tailed t-test (D, E and F).

doi:10.1371/journal.pone.0151147.g004

production *in vitro* but showed potential problems during clinical trials. Volunteers endured many adverse effects including headache, skin cancer, and liver failure [60–62]. Researchers also tested GSMs that moderately regulate the Aβ species produced, for which the clinical trials are still in progress [63]. Unlike these secretase inhibitors and modulators, RAPO, its active fraction RAPO-1-3 and the functional representative constituent Onjisaponin B reduced the Aβ level without interfering with the enzymatic activities of secretases. There is also a certain amount of Onjisaponin B in RAPO-3-2 based on the UPLC-Q-TOF/MS analysis of RAPO-3-2 (S2H Fig). However, there are differences in the peak patterns of RAPO-1-3 and RAPO-3-2 (S2B and S2G Fig). The cytotoxicity introduced by RAPO-3-2 treatment may result from other constituents in the fraction, which requires further investigation, and prompted us to abandon testing the *in vivo* efficacy of RAPO-3-2. We are continuing to attempt to separate the Aβ-reducing activity and the cytotoxicity of RAPO-3-2.

According to a previous reports, saponins were enriched in ethanol or methanol fractions [64] and the BPI chromatogram of RAPO-3-2 supports this conclusion (S2G and S2H Fig).

Moreover, saponins were also presented in RAPO-1 and RAPO-1-3 (S2A–S2D Fig). Using a two-step column chromatography separation method, we identified the major constituents in RAPO-1-3. In the UPLC-Q-TOF/MS chromatogram (S2A and S2B Fig), the representative acyl saponins peaks were observed at UV 310 nm. The total 10 related components were characterized as acyl saponins from RAPO-1-3 based on accurate mass measurement (S2H Fig and S1 Table). Those enriched acyl saponins possess highly similar structures, which makes it remarkably difficult to discriminate each compound from the others and certainly made it difficult to obtain an accurate plasma concentration of Onjisaponin B after drug administration. Due to technical problems, it is not clear why the plasma concentration of Onjisaponin B after RAPO-1-3 treatment was 10-folds higher than that after Onjisaponin B treatment at the 30-minute time point alone. It is possible that other compounds in RAPO-1-3 may enhance the absorption of Onjisaponin B and that other many saponins such as Onjisaponin R, S and Ng with similar polarity to Onjisaponin B may interfere with the peak area of Onjisaponin B. In addition, Onjisaponin B may have a relatively short half-life *in vivo*, and there might be other compounds in RAPO-1-3 that may be converted into Onjisaponin B and help to maintain the plasma drug concentration *in vivo*. All those possibilities must be further investigated. The higher level of Onjisaponin B *in vivo* after acute administration with RAPO-1-3 than after Onjisaponin B treatment alone might also explain why RAPO-1-3-treated AD mice performed better in the Morris Water Maze than did the Onjisaponin B-treated group.

There is evidence that proteostasis is disturbed in the brains of AD carriers [65]. As an important part of protein homeostasis, protein degradation plays a vital role in cleaning misfolded proteins, aggregated proteins or proteins no longer in use [66, 67]. This process can be accomplished directly, by the proteasome, or through other mechanisms such as autophagy [67]. Further mechanistic studies show that, together with our finding that Onjisaponin B reduces the A $\beta$  level by promoting APP degradation, it is possible that the autophagy-related Atg7-dependent AMPK/mTOR pathway may also be involved in A $\beta$  clearance, as in previous reports [68, 69].

To introduce another possible target for the modulation of AD, the interaction between BACE1 and  $\gamma$ -secretase and their chemical blockers have recently been reported by our lab [19]. Here, we found that Onjisaponin B also functioned as a mild inhibitor of the PS1/BACE1 interaction. Interestingly, Onjisaponin B interferes with the PS1/BACE1 interaction in an immunoprecipitation assay, reduces their FRET efficiency and dose-dependently reduces PS1-NTF/BACE1 interaction signal in a Split-TEV reporter assay.

RAPO is traditionally believed to harbor nootropic and tranquilizing efficacy, and it has therefore been used historically in China as a medical herb for memory deficits and insomnia [20]. Studies showed that RAPO produced a neuro-protective effect in a Parkinson's disease model [70], improved learning and memory ability in Alzheimer's disease animal models [71], and exhibited anti-depressant [72] and anti-inflammatory [73] activity. The underlying mechanisms include enhancing choline acetyl-transferase activity and nerve growth factor secretion [74], promoting BDNF and TrkB expression [75], and activating the NF- $\kappa$ B pathway [76], etc. Here, we report that Onjisaponin B from RAPO reduces A $\beta$  production by promoting APP degradation. It is fascinating to find that such one natural product could exhibit multiple functions, and these results support the new paradigm of Multi-Target-Directed Ligands (MTDLs) [77–79].

## Supporting Information

**S1 Document. The individual identification report of the components in RAPO-1-3.**  
(PDF)

**S1 Fig. Total secreted A $\beta$  in HEK293/APP<sup>swe</sup> culture medium.** Cells were treated with 0.1, 0.3 and 1 mg/ml RAPO or its fractions for 8 hours as indicated (A), and cell viability was monitored in parallel (B). Data are presented as the mean  $\pm$  s.e.m. \*  $p < 0.05$ , \*\*  $p < 0.01$  and \*\*\*  $p < 0.001$ . One-way ANOVA with Bonferroni's multiple comparison test (A, B). (TIF)

**S2 Fig. RAPO-1-3 and RAPO-3-2 characterization.** (A) UPLC chromatogram of RAPO-1-3 at 310 nm. (B) BPI chromatogram of RAPO-1-3 in negative ion mode. (C) Chemical structures of saponins identified in RAPO-1-3. (D) EIC chromatogram of Onjisaponin B in RAPO-1-3. (E) EIC chromatogram of Onjisaponin B at 500  $\mu$ g/ml. (F) EIC chromatogram of Onjisaponin B at 100  $\mu$ g/ml. (G) BPI chromatogram of RAPO-3-2 in negative mode. (H) EIC chromatogram of Onjisaponin B in RAPO-3-2. (TIF)

**S3 Fig. Onjisaponin B does not affect BACE1 maturation or  $\gamma$ -secretase activity or the secretase expression level *in vitro*.** (A) Onjisaponin B (10  $\mu$ M) does not alter the level of mature BACE1. (B) No significant alteration in the C99 processing pattern in the presence of 10  $\mu$ M Onjisaponin B. (C) mRNA levels of APP, BACE and  $\gamma$ -secretase components upon 10  $\mu$ M Onjisaponin B treatment. Data are presented as the mean  $\pm$  s.e.m. \*  $p < 0.05$ , \*\*  $p < 0.01$  and \*\*\*  $p < 0.001$ . One-way ANOVA with Bonferroni's multiple comparison test (C). (TIF)

**S4 Fig. Onjisaponin B interferes with PS1/BACE1 interaction.** (A) Onjisaponin B reduces PS1/BACE1 interaction. (B) Onjisaponin B reduces FRET efficiency of CFP-PS1/BACE1-YFP. (C) Onjisaponin B does not interfere with PS1 internal FRET efficiency. (D) Onjisaponin B dose-dependently reduces PS1-NTF/BACE1 interaction in Split-TEV luminescent reporter assay. Data are presented as the mean  $\pm$  s.e.m. \*  $p < 0.05$ , \*\*  $p < 0.01$  and \*\*\*  $p < 0.001$ . One-way ANOVA with Bonferroni's multiple comparison test (B, C) and one-way ANOVA with the Holm-Sidak multiple comparison test (D). (TIF)

**S5 Fig. Mouse body weight during compound administration, probe trial data at day 8 and representative images of brain slice immunostained with A $\beta$  and astrocyte.** (A) Monthly body weight. (B) Latency to platform in the probe trial. (C) Time spent in the target quadrant for each group. Data are presented as the mean  $\pm$  s.e.m. \*  $p < 0.05$ , \*\*  $p < 0.01$  and \*\*\*  $p < 0.001$ . Two-way ANOVA with Bonferroni's multiple comparison test (A, C), one-way ANOVA with Bonferroni's multiple comparison test (B). (D) More representative images of amyloid- $\beta$  plaques in APP/PS1 mice immunostained with A $\beta$  antibody 6E10 in coronal mouse brain cryo-sections. (TIF)

**S1 Protocol. Supplementary material and methods.**  
(DOCX)

**S1 Table. Main compounds identified in RAPO-1-3 by UPLC-ESI-Q-TOF/MS.**  
(PDF)

**S2 Table. The detailed information of the main peak areas in RAPO-1-3.**  
(PDF)

## Acknowledgments

We thank Dr Raphael Kopan (Washington University) for the myc-Notch $\Delta$ E plasmid. We appreciate Sanofi-Aventis Research and Development for providing us with the Split-TEV

assay constructs and HEK293MSR. We thank all members in our laboratory for advice and sharing reagents.

## Author Contributions

Conceived and designed the experiments: XL JZ GP. Performed the experiments: XL JC DQ WL XW YH. Analyzed the data: XL WL. Contributed reagents/materials/analysis tools: YY XY CZ. Wrote the paper: XL JZ GP.

## References

1. Alzheimer's Association. Alzheimer's Association Report 2015 Alzheimer's disease facts and figures. *Alzheimers & Dementia*. 2015; 11(3):332–84. doi: [10.1016/j.jalz.2015.02.003](https://doi.org/10.1016/j.jalz.2015.02.003) ISI:000352465100012.
2. Parihar MS, Hemnani T. Alzheimer's disease pathogenesis and therapeutic interventions. *Journal of clinical neuroscience: official journal of the Neurosurgical Society of Australasia*. 2004; 11(5):456–67. Epub 2004/06/05. doi: [10.1016/j.jocn.2003.12.007](https://doi.org/10.1016/j.jocn.2003.12.007) PMID: [15177383](https://pubmed.ncbi.nlm.nih.gov/15177383/).
3. Sommer B. Alzheimer's disease and the amyloid cascade hypothesis: ten years on. *Current opinion in pharmacology*. 2002; 2(1):87–92. Epub 2002/01/12. PMID: [11786314](https://pubmed.ncbi.nlm.nih.gov/11786314/).
4. Hardy JA, Higgins GA. Alzheimer's disease: the amyloid cascade hypothesis. *Science*. 1992; 256(5054):184–5. Epub 1992/04/10. PMID: [1566067](https://pubmed.ncbi.nlm.nih.gov/1566067/).
5. Tagawa K, Kunishita T, Maruyama K, Yoshikawa K, Kominami E, Tsuchiya T, et al. Alzheimer's disease amyloid beta-clipping enzyme (APP secretase): identification, purification, and characterization of the enzyme. *Biochemical and biophysical research communications*. 1991; 177(1):377–87. Epub 1991/05/31. PMID: [1645961](https://pubmed.ncbi.nlm.nih.gov/1645961/).
6. Tischer E, Cordell B. Beta-amyloid precursor protein. Location of transmembrane domain and specificity of gamma-secretase cleavage. *The Journal of biological chemistry*. 1996; 271(36):21914–9. Epub 1996/09/06. PMID: [8702994](https://pubmed.ncbi.nlm.nih.gov/8702994/).
7. Giannakopoulos P, Hof PR, Mottier S, Michel JP, Bouras C. Neuropathological Changes in the Cerebral-Cortex of 1258 Cases from a Geriatric Hospital—Retrospective Clinicopathological Evaluation of a 10-Year Autopsy Population. *Acta neuropathologica*. 1994; 87(5):456–68. ISI:A1994NJ77300004. PMID: [8059598](https://pubmed.ncbi.nlm.nih.gov/8059598/)
8. Heinonen O, Soininen H, Sorvari H, Kosunen O, Paljarvi L, Koivisto E, et al. Loss of synaptophysin-like immunoreactivity in the hippocampal formation is an early phenomenon in Alzheimer's disease. *Neuroscience*. 1995; 64(2):375–84. Epub 1995/01/01. PMID: [7700527](https://pubmed.ncbi.nlm.nih.gov/7700527/).
9. Mitani Y, Yarimizu J, Saita K, Uchino H, Akashiba H, Shitaka Y, et al. Differential Effects between gamma-Secretase Inhibitors and Modulators on Cognitive Function in Amyloid Precursor Protein-Transgenic and Nontransgenic Mice. *Journal of Neuroscience*. 2012; 32(6):2037–50. doi: [10.1523/Jneurosci.4264-11.2012](https://doi.org/10.1523/Jneurosci.4264-11.2012) ISI:000300207900016. PMID: [22323718](https://pubmed.ncbi.nlm.nih.gov/22323718/)
10. Imbimbo BP, Giardina GA. gamma-secretase inhibitors and modulators for the treatment of Alzheimer's disease: disappointments and hopes. *Current topics in medicinal chemistry*. 2011; 11(12):1555–70. Epub 2011/04/23. PMID: [21510832](https://pubmed.ncbi.nlm.nih.gov/21510832/).
11. De Strooper B, Chavez Gutierrez L. Learning by failing: ideas and concepts to tackle gamma-secretases in Alzheimer's disease and beyond. *Annual review of pharmacology and toxicology*. 2015; 55:419–37. Epub 2014/10/09. doi: [10.1146/annurev-pharmtox-010814-124309](https://doi.org/10.1146/annurev-pharmtox-010814-124309) PMID: [25292430](https://pubmed.ncbi.nlm.nih.gov/25292430/).
12. Nunan J, Williamson NA, Hill AF, Sernee MF, Masters CL, Small DH. Proteasome-mediated degradation of the C-terminus of the Alzheimer's disease beta-amyloid protein precursor: effect of C-terminal truncation on production of beta-amyloid protein. *Journal of neuroscience research*. 2003; 74(3):378–85. Epub 2003/11/05. doi: [10.1002/jnr.10646](https://doi.org/10.1002/jnr.10646) PMID: [14598314](https://pubmed.ncbi.nlm.nih.gov/14598314/).
13. El Ayadi A, Stieren ES, Barral JM, Boehning D. Ubiquitin-1 regulates amyloid precursor protein maturation and degradation by stimulating K63-linked polyubiquitination of lysine 688. *Proceedings of the National Academy of Sciences of the United States of America*. 2012; 109(33):13416–21. Epub 2012/08/01. doi: [10.1073/pnas.1206786109](https://doi.org/10.1073/pnas.1206786109) PMID: [22847417](https://pubmed.ncbi.nlm.nih.gov/22847417/); PubMed Central PMCID: PMC3421158.
14. Agholme L, Hallbeck M, Benedikz E, Marcusson J, Kagedal K. Amyloid-beta secretion, generation, and lysosomal sequestration in response to proteasome inhibition: involvement of autophagy. *Journal of Alzheimer's disease: JAD*. 2012; 31(2):343–58. Epub 2012/05/05. doi: [10.3233/JAD-2012-120001](https://doi.org/10.3233/JAD-2012-120001) PMID: [22555375](https://pubmed.ncbi.nlm.nih.gov/22555375/).
15. Richterruoff B, Heinemeyer W, Wolf DH. The Proteasome Multicatalytic Multifunctional Proteinase—Invivo Function in the Ubiquitin-Dependent N-End Rule Pathway of Protein-Degradation in Eukaryotes.

- FEBS letters. 1992; 302(2):192–6. doi: [10.1016/0014-5793\(92\)80438-M](https://doi.org/10.1016/0014-5793(92)80438-M) ISI:A1992HU89700023. PMID: [1321727](https://pubmed.ncbi.nlm.nih.gov/1321727/)
16. Hiltunen M, Lu A, Thomas AV, Romano DM, Kim M, Jones PB, et al. Ubiquilin 1 modulates amyloid precursor protein trafficking and Abeta secretion. *The Journal of biological chemistry*. 2006; 281(43):32240–53. Epub 2006/09/02. doi: [10.1074/jbc.M603106200](https://doi.org/10.1074/jbc.M603106200) PMID: [16945923](https://pubmed.ncbi.nlm.nih.gov/16945923/).
  17. Watanabe T, Hikichi Y, Willuweit A, Shintani Y, Horiguchi T. FBL2 regulates amyloid precursor protein (APP) metabolism by promoting ubiquitination-dependent APP degradation and inhibition of APP endocytosis. *The Journal of neuroscience: the official journal of the Society for Neuroscience*. 2012; 32(10):3352–65. Epub 2012/03/09. doi: [10.1523/JNEUROSCI.5659-11.2012](https://doi.org/10.1523/JNEUROSCI.5659-11.2012) PMID: [22399757](https://pubmed.ncbi.nlm.nih.gov/22399757/).
  18. Baranello RJ, Bharani KL, Padmaraju V, Chopra N, Lahiri DK, Greig NH, et al. Amyloid-beta protein clearance and degradation (ABCD) pathways and their role in Alzheimer's disease. *Current Alzheimer research*. 2015; 12(1):32–46. Epub 2014/12/20. PMID: [25523424](https://pubmed.ncbi.nlm.nih.gov/25523424/).
  19. Cui J, Wang X, Li X, Wang X, Zhang C, Li W, et al. Targeting the  $\gamma$ - $\beta$ -secretase interaction reduces  $\beta$ -amyloid generation and ameliorates Alzheimer's disease-related pathogenesis. *Cell Discovery*. 2015; 1:15021. doi: [10.1038/celldisc.2015.21](https://doi.org/10.1038/celldisc.2015.21)<http://www.nature.com/articles/celldisc201521#supplementary-information>.
  20. Lin ZH, Gu J, Xiu J, Mi TY, Dong J, Tiwari JK. Traditional Chinese Medicine for Senile Dementia. *Evid-Based Compl Alt*. 2012;1–13. Artn 692621 doi: [10.1155/2012/692621](https://doi.org/10.1155/2012/692621) ISI:000294620700001.
  21. May BH, Lu C, Lu Y, Zhang AL, Xue CC. Chinese herbs for memory disorders: a review and systematic analysis of classical herbal literature. *Journal of acupuncture and meridian studies*. 2013; 6(1):2–11. Epub 2013/02/26. doi: [10.1016/j.jams.2012.11.009](https://doi.org/10.1016/j.jams.2012.11.009) PMID: [23433049](https://pubmed.ncbi.nlm.nih.gov/23433049/).
  22. Sun ZK, Yang HQ, Chen SD. Traditional Chinese medicine: a promising candidate for the treatment of Alzheimer's disease. *Translational neurodegeneration*. 2013; 2(1):6. Epub 2013/03/01. doi: [10.1186/2047-9158-2-6](https://doi.org/10.1186/2047-9158-2-6) PMID: [23445907](https://pubmed.ncbi.nlm.nih.gov/23445907/); PubMed Central PMCID: PMC3599149.
  23. Liu P, Kong MW, Yuan SH, Liu JF, Wang P. History and Experience: A Survey of Traditional Chinese Medicine Treatment for Alzheimer's Disease. *Evid-Based Compl Alt*. 2014. Artn 642128 doi: [10.1155/2014/642128](https://doi.org/10.1155/2014/642128) ISI:000330903400001.
  24. Wang Y, Wang Y, Sui Y, Yu HS, Shen XH, Chen SD, et al. The Combination of Aricept with a Traditional Chinese Medicine Formula, Smart Soup, May Be a Novel Way to Treat Alzheimer's Disease. *Journal of Alzheimers Disease*. 2015; 45(4):1185–95. doi: [10.3233/Jad-143183](https://doi.org/10.3233/Jad-143183) ISI:000352819200018.
  25. Zhang H, Han T, Zhang L, Yu CH, Wan DG, Rahman K, et al. Effects of tenuifolin extracted from radix polygalae on learning and memory: a behavioral and biochemical study on aged and amnesic mice. *Phytomedicine: international journal of phytotherapy and phytopharmacology*. 2008; 15(8):587–94. Epub 2008/02/22. doi: [10.1016/j.phymed.2007.12.004](https://doi.org/10.1016/j.phymed.2007.12.004) PMID: [18289838](https://pubmed.ncbi.nlm.nih.gov/18289838/).
  26. Hou YJ, Wang Y, Zhao J, Li XH, Cui J, Ding JQ, et al. Smart Soup, a Traditional Chinese Medicine Formula, Ameliorates Amyloid Pathology and Related Cognitive Deficits. *PloS one*. 2014; 9(11). ARTN e111215doi: [10.1371/journal.pone.0111215](https://doi.org/10.1371/journal.pone.0111215) ISI:000345250400015.
  27. Vorhees CV, Williams MT. Morris water maze: procedures for assessing spatial and related forms of learning and memory. *Nature protocols*. 2006; 1(2):848–58. Epub 2007/04/05. doi: [10.1038/nprot.2006.116](https://doi.org/10.1038/nprot.2006.116) PMID: [17406317](https://pubmed.ncbi.nlm.nih.gov/17406317/); PubMed Central PMCID: PMC2895266.
  28. Wang X, Cui J, Li W, Zeng X, Zhao J, Pei G. gamma-Secretase Modulators and Inhibitors Induce Different Conformational Changes of Presenilin 1 Revealed by FLIM and FRET. *Journal of Alzheimer's disease: JAD*. 2015; 47(4):927–37. Epub 2015/09/25. doi: [10.3233/JAD-150313](https://doi.org/10.3233/JAD-150313) PMID: [26401772](https://pubmed.ncbi.nlm.nih.gov/26401772/).
  29. Hou Y, Wang Y, Zhao J, Li X, Cui J, Ding J, et al. Smart Soup, a traditional Chinese medicine formula, ameliorates amyloid pathology and related cognitive deficits. *PloS one*. 2014; 9(11):e111215. Epub 2014/11/12. doi: [10.1371/journal.pone.0111215](https://doi.org/10.1371/journal.pone.0111215) PMID: [25386946](https://pubmed.ncbi.nlm.nih.gov/25386946/); PubMed Central PMCID: PMC4227681.
  30. Ni Y, Zhao X, Bao G, Zou L, Teng L, Wang Z, et al. Activation of beta2-adrenergic receptor stimulates gamma-secretase activity and accelerates amyloid plaque formation. *Nature medicine*. 2006; 12(12):1390–6. Epub 2006/11/23. doi: [10.1038/nm1485](https://doi.org/10.1038/nm1485) PMID: [17115048](https://pubmed.ncbi.nlm.nih.gov/17115048/).
  31. Yin YI, Bassit B, Zhu L, Yang X, Wang CY, Li YM. gamma-secretase substrate concentration modulates the A beta 42/A beta 40 ratio. *Journal of Biological Chemistry*. 2007; 282(32):23639–44. doi: [10.1074/jbc.M704601200](https://doi.org/10.1074/jbc.M704601200) ISI:000248577500066. PMID: [17556361](https://pubmed.ncbi.nlm.nih.gov/17556361/)
  32. Liu X, Zhao X, Zeng X, Bossers K, Swaab DF, Zhao J, et al. beta-arrestin1 regulates gamma-secretase complex assembly and modulates amyloid-beta pathology. *Cell research*. 2013; 23(3):351–65. Epub 2012/12/05. doi: [10.1038/cr.2012.167](https://doi.org/10.1038/cr.2012.167) PMID: [23208420](https://pubmed.ncbi.nlm.nih.gov/23208420/); PubMed Central PMCID: PMC3587707.
  33. Citron M, Oltsersdorf T, Haass C, McConlogue L, Hung AY, Seubert P, et al. Mutation of the beta-amyloid precursor protein in familial Alzheimer's disease increases beta-protein production. *Nature*. 1992; 360(6405):672–4. Epub 1992/12/17. doi: [10.1038/360672a0](https://doi.org/10.1038/360672a0) PMID: [1465129](https://pubmed.ncbi.nlm.nih.gov/1465129/).



34. Jankowsky JL, Slunt HH, Ratovitski T, Jenkins NA, Copeland NG, Borchelt DR. Co-expression of multiple transgenes in mouse CNS: a comparison of strategies. *Biomolecular engineering*. 2001; 17(6):157–65. Epub 2001/05/05. PMID: [11337275](#).
35. Garcia-Alloza M, Robbins EM, Zhang-Nunes SX, Purcell SM, Betensky RA, Raju S, et al. Characterization of amyloid deposition in the APP<sup>swe</sup>/PS1<sup>dE9</sup> mouse model of Alzheimer disease. *Neurobiology of disease*. 2006; 24(3):516–24. Epub 2006/10/13. doi: [10.1016/j.nbd.2006.08.017](#) PMID: [17029828](#).
36. Reiserer RS, Harrison FE, Syverud DC, McDonald MP. Impaired spatial learning in the APP<sup>swe</sup> + PSEN1<sup>DeltaE9</sup> bigenic mouse model of Alzheimer's disease. *Genes, brain, and behavior*. 2007; 6(1):54–65. Epub 2007/01/20. doi: [10.1111/j.1601-183X.2006.00221.x](#) PMID: [17233641](#).
37. Morris R. Developments of a water-maze procedure for studying spatial learning in the rat. *Journal of neuroscience methods*. 1984; 11(1):47–60. Epub 1984/05/01. PMID: [6471907](#).
38. Gallagher JJ, Minogue AM, Lynch MA. Impaired performance of female APP/PS1 mice in the Morris water maze is coupled with increased Abeta accumulation and microglial activation. *Neuro-degenerative diseases*. 2013; 11(1):33–41. Epub 2012/05/26. doi: [10.1159/000337458](#) PMID: [22627185](#).
39. Walsh DM, Klyubin I, Fadeeva JV, Cullen WK, Anwyl R, Wolfe MS, et al. Naturally secreted oligomers of amyloid beta protein potently inhibit hippocampal long-term potentiation in vivo. *Nature*. 2002; 416(6880):535–9. Epub 2002/04/05. doi: [10.1038/416535a](#) PMID: [11932745](#).
40. Lesne S, Koh MT, Kotilinek L, Kaye R, Glabe CG, Yang A, et al. A specific amyloid-beta protein assembly in the brain impairs memory. *Nature*. 2006; 440(7082):352–7. Epub 2006/03/17. doi: [10.1038/nature04533](#) PMID: [16541076](#).
41. Younkin SG. Processing of the Alzheimer's disease beta A4 amyloid protein precursor (APP). *Brain Pathol*. 1991; 1(4):253–62. Epub 1991/07/01. PMID: [1669715](#).
42. Bunnell WL, Pham HV, Glabe CG. gamma-secretase cleavage is distinct from endoplasmic reticulum degradation of the transmembrane domain of the amyloid precursor protein. *The Journal of biological chemistry*. 1998; 273(48):31947–55. Epub 1998/11/21. PMID: [9822665](#).
43. Murphy MP, Uljon SN, Fraser PE, Fauq A, Lookingbill HA, Findlay KA, et al. Presenilin 1 regulates pharmacologically distinct gamma-secretase activities. Implications for the role of presenilin in gamma-secretase cleavage. *The Journal of biological chemistry*. 2000; 275(34):26277–84. Epub 2000/05/19. doi: [10.1074/jbc.M002812200](#) PMID: [10816583](#).
44. Murphy MP, Hickman LJ, Eckman CB, Uljon SN, Wang R, Golde TE. gamma-Secretase, evidence for multiple proteolytic activities and influence of membrane positioning of substrate on generation of amyloid beta peptides of varying length. *Journal of Biological Chemistry*. 1999; 274(17):11914–23. doi: [10.1074/jbc.274.17.11914](#) ISI:000079834800068. PMID: [10207012](#)
45. Yin YI, Bassit B, Zhu L, Yang X, Wang C, Li YM. {gamma}-Secretase Substrate Concentration Modulates the Abeta42/Abeta40 Ratio: IMPLICATIONS FOR ALZHEIMER DISEASE. *The Journal of biological chemistry*. 2007; 282(32):23639–44. Epub 2007/06/09. doi: [10.1074/jbc.M704601200](#) PMID: [17556361](#).
46. Bai X, Weitz JI, Gross PL. Leukocyte urokinase plasminogen activator receptor and PSGL1 play a role in endogenous arterial fibrinolysis. *Thromb Haemost*. 2009; 102(6):1212–8. Epub 2009/12/08. doi: [10.1160/TH09-01-0038](#) PMID: [19967153](#).
47. Lichtenthaler SF, Dominguez D, Westmeyer GG, Reiss K, Haass C, Saftig P, et al. The cell adhesion protein P-selectin glycoprotein ligand-1 is a substrate for the aspartyl protease BACE1. *Journal of Biological Chemistry*. 2003; 278(49):48713–9. doi: [10.1074/jbc.M303861200](#) ISI:000186829000026. PMID: [14507929](#)
48. Thinakaran G, Teplow DB, Siman R, Greenberg B, Sisodia SS. Metabolism of the "Swedish" amyloid precursor protein variant in neuro2a (N2a) cells. Evidence that cleavage at the "beta-secretase" site occurs in the golgi apparatus. *The Journal of biological chemistry*. 1996; 271(16):9390–7. Epub 1996/04/19. PMID: [8621605](#).
49. Nunan J, Shearman MS, Checler F, Cappai R, Evin G, Beyreuther K, et al. The C-terminal fragment of the Alzheimer's disease amyloid protein precursor is degraded by a proteasome-dependent mechanism distinct from gamma-secretase. *European journal of biochemistry / FEBS*. 2001; 268(20):5329–36. Epub 2001/10/19. PMID: [11606195](#).
50. Steinhilb ML, Turner RS, Gaut JR. ELISA analysis of beta-secretase cleavage of the Swedish amyloid precursor protein in the secretory and endocytic pathways. *Journal of neurochemistry*. 2002; 80(6):1019–28. Epub 2002/04/16. PMID: [11953452](#).
51. Thinakaran G, Koo EH. Amyloid precursor protein trafficking, processing, and function. *The Journal of biological chemistry*. 2008; 283(44):29615–9. Epub 2008/07/25. doi: [10.1074/jbc.R800019200](#) PMID: [18650430](#); PubMed Central PMCID: PMC2573065.

52. Jung ES, Hong H, Kim C, Mook-Jung I. Acute ER stress regulates amyloid precursor protein processing through ubiquitin-dependent degradation. *Scientific reports*. 2015; 5:8805. Epub 2015/03/06. doi: [10.1038/srep08805](https://doi.org/10.1038/srep08805) PMID: [25740315](https://pubmed.ncbi.nlm.nih.gov/25740315/).
53. Cavieres VA, Gonzalez A, Munoz VC, Yefi CP, Bustamante HA, Barraza RR, et al. Tetrahydrohydropyridin Inhibits the Proteolytic Processing of Amyloid Precursor Protein and Enhances Its Degradation by Atg5-Dependent Autophagy. *PLoS one*. 2015; 10(8):e0136313. Epub 2015/08/27. doi: [10.1371/journal.pone.0136313](https://doi.org/10.1371/journal.pone.0136313) PMID: [26308941](https://pubmed.ncbi.nlm.nih.gov/26308941/); PubMed Central PMCID: [PMC4550396](https://pubmed.ncbi.nlm.nih.gov/PMC4550396/).
54. Lee DH, Goldberg AL. Selective inhibitors of the proteasome-dependent and vacuolar pathways of protein degradation in *Saccharomyces cerevisiae*. *The Journal of biological chemistry*. 1996; 271(44):27280–4. Epub 1996/11/01. PMID: [8910302](https://pubmed.ncbi.nlm.nih.gov/8910302/).
55. De Strooper B, Annaert W, Cupers P, Saftig P, Craessaerts K, Mumm JS, et al. A presenilin-1-dependent gamma-secretase-like protease mediates release of Notch intracellular domain. *Nature*. 1999; 398(6727):518–22. Epub 1999/04/17. doi: [10.1038/19083](https://doi.org/10.1038/19083) PMID: [10206645](https://pubmed.ncbi.nlm.nih.gov/10206645/).
56. Wehr MC, Laage R, Bolz U, Fischer TM, Grunewald S, Scheek S, et al. Monitoring regulated protein-protein interactions using split TEV. *Nat Methods*. 2006; 3(12):985–93. doi: [10.1038/Nmeth967](https://doi.org/10.1038/Nmeth967) ISI:000242213900017. PMID: [17072307](https://pubmed.ncbi.nlm.nih.gov/17072307/)
57. Jardanhazi-Kurutz D, Kummer MP, Terwel D, Vogel K, Dyrks T, Thiele A, et al. Induced LC degeneration in APP/PS1 transgenic mice accelerates early cerebral amyloidosis and cognitive deficits. *Neurochemistry international*. 2010; 57(4):375–82. Epub 2010/02/11. doi: [10.1016/j.neuint.2010.02.001](https://doi.org/10.1016/j.neuint.2010.02.001) PMID: [20144675](https://pubmed.ncbi.nlm.nih.gov/20144675/).
58. Weitz TM, Gate D, Rezai-Zadeh K, Town T. MyD88 Is Dispensable for Cerebral Amyloidosis and Neuroinflammation in APP/PS1 Transgenic Mice. *The American journal of pathology*. 2014; 184(11):2855–61. Epub 2014/09/02. doi: [10.1016/j.ajpath.2014.07.004](https://doi.org/10.1016/j.ajpath.2014.07.004) PMID: [25174876](https://pubmed.ncbi.nlm.nih.gov/25174876/); PubMed Central PMCID: [PMC4215030](https://pubmed.ncbi.nlm.nih.gov/PMC4215030/).
59. West S, Bhugra P. Emerging drug targets for Abeta and tau in Alzheimer's disease: a systematic review. *British journal of clinical pharmacology*. 2015. Epub 2015/03/11. doi: [10.1111/bcp.12621](https://doi.org/10.1111/bcp.12621) PMID: [25753046](https://pubmed.ncbi.nlm.nih.gov/25753046/).
60. Geling A, Steiner H, Willem M, Bally-Cuif L, Haass C. A gamma-secretase inhibitor blocks Notch signaling in vivo and causes a severe neurogenic phenotype in zebrafish. *EMBO reports*. 2002; 3(7):688–94. Epub 2002/07/09. doi: [10.1093/embo-reports/kvf124](https://doi.org/10.1093/embo-reports/kvf124) PMID: [12101103](https://pubmed.ncbi.nlm.nih.gov/12101103/); PubMed Central PMCID: [PMC1084181](https://pubmed.ncbi.nlm.nih.gov/PMC1084181/).
61. Svedruzic ZM, Popovic K, Sendula-Jengic V. Modulators of gamma-secretase activity can facilitate the toxic side-effects and pathogenesis of Alzheimer's disease. *PLoS one*. 2013; 8(1):e50759. Epub 2013/01/12. doi: [10.1371/journal.pone.0050759](https://doi.org/10.1371/journal.pone.0050759) PMID: [23308095](https://pubmed.ncbi.nlm.nih.gov/23308095/); PubMed Central PMCID: [PMC3538728](https://pubmed.ncbi.nlm.nih.gov/PMC3538728/).
62. Villegas S. Alzheimer's disease: New therapeutic strategies. *Medicina clinica*. 2015; 145(2):76–83. doi: [10.1016/j.medcli.2014.05.023](https://doi.org/10.1016/j.medcli.2014.05.023) ISI:000358025500006. PMID: [25245784](https://pubmed.ncbi.nlm.nih.gov/25245784/)
63. Tomita T. [Development of Alzheimer's disease treatment based on the molecular mechanism of gamma-secretase activity]. *Rinsho shinkeigaku = Clinical neurology*. 2012; 52(11):1165–7. Epub 2012/12/01. PMID: [23196551](https://pubmed.ncbi.nlm.nih.gov/23196551/).
64. Jiang Yong LJ, Tu Peng Fei., inventor; Fenghua Wang, assignee. Effective place of polygala root and its use. China patent CN 1315497C. 2005 2005-07-20.
65. Di Domenico F, Coccia R, Cocciolo A, Murphy MP, Cenini G, Head E, et al. Impairment of proteostasis network in Down syndrome prior to the development of Alzheimer's disease neuropathology: redox proteomics analysis of human brain. *Biochimica et biophysica acta*. 2013; 1832(8):1249–59. Epub 2013/04/23. doi: [10.1016/j.bbadis.2013.04.013](https://doi.org/10.1016/j.bbadis.2013.04.013) PMID: [23603808](https://pubmed.ncbi.nlm.nih.gov/23603808/); PubMed Central PMCID: [PMC3940071](https://pubmed.ncbi.nlm.nih.gov/PMC3940071/).
66. Nijholt DA, De Kimpe L, Elfrink HL, Hoozemans JJ, Scheper W. Removing protein aggregates: the role of proteolysis in neurodegeneration. *Current medicinal chemistry*. 2011; 18(16):2459–76. Epub 2011/05/17. PMID: [21568912](https://pubmed.ncbi.nlm.nih.gov/21568912/).
67. McKinnon C, Tabrizi SJ. The ubiquitin-proteasome system in neurodegeneration. *Antioxidants & redox signaling*. 2014; 21(17):2302–21. Epub 2014/01/21. doi: [10.1089/ars.2013.5802](https://doi.org/10.1089/ars.2013.5802) PMID: [24437518](https://pubmed.ncbi.nlm.nih.gov/24437518/).
68. Zhao H, Wang ZC, Wang KF, Chen XY. Abeta peptide secretion is reduced by Radix Polygalae-induced autophagy via activation of the AMPK/mTOR pathway. *Molecular medicine reports*. 2015; 12(2):2771–6. Epub 2015/05/16. doi: [10.3892/mmr.2015.3781](https://doi.org/10.3892/mmr.2015.3781) PMID: [25976650](https://pubmed.ncbi.nlm.nih.gov/25976650/).
69. Wu AG, Wong VK, Xu SW, Chan WK, Ng CI, Liu L, et al. Onjisaponin B derived from Radix Polygalae enhances autophagy and accelerates the degradation of mutant alpha-synuclein and huntingtin in PC-12 cells. *International journal of molecular sciences*. 2013; 14(11):22618–41. Epub 2013/11/20. doi: [10.3390/ijms141122618](https://doi.org/10.3390/ijms141122618) PMID: [24248062](https://pubmed.ncbi.nlm.nih.gov/24248062/); PubMed Central PMCID: [PMC3856081](https://pubmed.ncbi.nlm.nih.gov/PMC3856081/).
70. Choi JG, Kim HG, Kim MC, Yang WM, Huh Y, Kim SY, et al. Polygalae radix inhibits toxin-induced neuronal death in the Parkinson's disease models. *Journal of ethnopharmacology*. 2011; 134(2):414–21. Epub 2011/01/05. doi: [10.1016/j.jep.2010.12.030](https://doi.org/10.1016/j.jep.2010.12.030) PMID: [21195155](https://pubmed.ncbi.nlm.nih.gov/21195155/).

71. Karakida F, Ikeya Y, Tsunakawa M, Yamaguchi T, Ikarashi Y, Takeda S, et al. Cerebral protective and cognition-improving effects of sinapic acid in rodents. *Biological & pharmaceutical bulletin*. 2007; 30(3):514–9. doi: [10.1248/Bpb.30.514](https://doi.org/10.1248/Bpb.30.514) ISI:000245938200021.
72. Liu P, Hu Y, Guo DH, Wang DX, Tu HH, Ma L, et al. Potential antidepressant properties of Radix Polygalae (Yuan Zhi). *Phytomedicine: international journal of phytotherapy and phytopharmacology*. 2010; 17(10):794–9. Epub 2010/06/15. doi: [10.1016/j.phymed.2010.01.004](https://doi.org/10.1016/j.phymed.2010.01.004) PMID: [20541923](https://pubmed.ncbi.nlm.nih.gov/20541923/).
73. Oh JJ, Kim SJ. Inhibitory Effect of the root of Polygala tenuifolia on Bradykinin and COX 2-Mediated Pain and Inflammatory Activity. *Trop J Pharm Res*. 2013; 12(5):755–9. doi: [10.4314/tjpr.v12i5.14](https://doi.org/10.4314/tjpr.v12i5.14) ISI:000325748700014.
74. Yabe T, Iizuka S, Komatsu Y, Yamada H. Enhancements of choline acetyltransferase activity and nerve growth factor secretion by Polygalae radix-extract containing active ingredients in Kami-untan-to. *Phytomedicine: international journal of phytotherapy and phytopharmacology*. 1997; 4(3):199–205. Epub 1997/09/01. doi: [10.1016/S0944-7113\(97\)80068-2](https://doi.org/10.1016/S0944-7113(97)80068-2) PMID: [23195476](https://pubmed.ncbi.nlm.nih.gov/23195476/).
75. Sun Y, Xie TT, Wang DX, Liu P. [Effect of Polygala tenuifolia Willd YZ-50 on the mRNA expression of brain-derived neurotrophic factor and its receptor TrkB in rats with chronic stress depression]. *Nan fang yi ke da xue xue bao = Journal of Southern Medical University*. 2009; 29(6):1199–203. Epub 2009/09/04. PMID: [19726361](https://pubmed.ncbi.nlm.nih.gov/19726361/).
76. Cheong MH, Lee SR, Yoo HS, Jeong JW, Kim GY, Kim WJ, et al. Anti-inflammatory effects of Polygala tenuifolia root through inhibition of NF-kappaB activation in lipopolysaccharide-induced BV2 microglial cells. *Journal of ethnopharmacology*. 2011; 137(3):1402–8. Epub 2011/08/23. doi: [10.1016/j.jep.2011.08.008](https://doi.org/10.1016/j.jep.2011.08.008) PMID: [21856398](https://pubmed.ncbi.nlm.nih.gov/21856398/).
77. Bajda M, Guzior N, Ignasik M, Malawska B. Multi-target-directed ligands in Alzheimer's disease treatment. *Current medicinal chemistry*. 2011; 18(32):4949–75. Epub 2011/11/05. PMID: [22050745](https://pubmed.ncbi.nlm.nih.gov/22050745/).
78. Agis-Torres A, Sollhuber M, Fernandez M, Sanchez-Montero JM. Multi-Target-Directed Ligands and other Therapeutic Strategies in the Search of a Real Solution for Alzheimer's Disease. *Curr Neuropharmacol*. 2014; 12(1):2–36. doi: [10.2174/1570159x113116660047](https://doi.org/10.2174/1570159x113116660047) ISI:000331461900002. PMID: [24533013](https://pubmed.ncbi.nlm.nih.gov/24533013/)
79. Guzior N, Wieckowska A, Panek D, Malawska B. Recent Development of Multifunctional Agents as Potential Drug Candidates for the Treatment of Alzheimer's Disease. *Current medicinal chemistry*. 2015; 22(3):373–404. ISI:000349386900007. PMID: [25386820](https://pubmed.ncbi.nlm.nih.gov/25386820/)